The Novel Adipokine Gremlin 1 Antagonizes Insulin Action and Is Increased in Type 2 Diabetes and NAFLD/NASH

Shahram Hedjazifar,[1] Roxana Khatib Shahidi,[1] Ann Hammarstedt,[1] Laurianne Bonnet,[1,2] Christopher Church,[3] Jeremie Boucher,[1,2,4] Matthias Blüher,[5] and Ulf Smith[1]

Diabetes 2020;69:331–341 | https://doi.org/10.2337/db19-0701

The BMP2/4 antagonist and novel adipokine Gremlin 1 is highly expressed in human adipose cells and increased in hypertrophic obesity. As a secreted antagonist, it inhibits the effect of BMP2/4 on adipose precursor cell commitment/differentiation. We examined mRNA levels of Gremlin 1 in key target tissues for insulin and also measured tissue and serum levels in several carefully phenotyped human cohorts. Gremlin 1 expression was high in adipose tissue, higher in visceral than in subcutaneous tissue, increased in obesity, and further increased in type 2 diabetes (T2D). A similar high expression was seen in liver biopsies, but expression was considerably lower in skeletal muscles. Serum levels were increased in obesity but most prominently in T2D. Transcriptional activation in both adipose tissue and liver as well as serum levels were strongly associated with markers of insulin resistance in vivo (euglycemic clamps and HOMA of insulin resistance), and the presence of nonalcoholic fatty liver disease (NAFLD) and nonalcoholic steatohepatitis (NASH). We also found Gremlin 1 to antagonize insulin signaling and action in human primary adipocytes, skeletal muscle, and liver cells. Thus, Gremlin 1 is a novel secreted insulin antagonist and biomarker as well as a potential therapeutic target in obesity and its complications T2D and NAFLD/NASH.

Obesity is the major driver of the rising prevalence of insulin resistance/type 2 diabetes (T2D) and related complications, including cardiovascular disease, nonalcoholic fatty liver disease (NAFLD), and its severe form, nonalcoholic steatohepatitis (NASH). Hypertrophic obesity with expanded adipose cells is closely associated with insulin resistance and an inflamed and dysregulated subcutaneous adipose tissue with reduced ability to store excess fat and, instead, promoting ectopic lipid accumulation in other tissues including liver and skeletal muscle (1). An attractive therapeutic approach to treat hypertrophic obesity is to promote browning of white adipose tissue to increase mitochondrial biogenesis and whole-body energy expenditure. However, there is also a need for novel insulin-sensitizing drugs to treat insulin resistance/T2D independent of effects on obesity.

We and others have earlier demonstrated that increased adipose tissue and circulating levels of BMP4 can counteract obesity by promoting browning of white adipose tissue (1,2). However, both adipose tissue and serum levels of BMP4 are actually increased in obesity in man and in mice (3–5), while beige/brown adipose cell markers are reduced in obesity.

An important reason for this is that the endogenous BMP antagonists are also increased. Human adipose tissue expresses several antagonists including Gremlin 1, Noggin, Chordin-like 1, Follistatin, and BAMBI (3) but we found the secreted BMP2/4 antagonist Gremlin 1 to be the major endogenous antagonist inhibiting BMP4-induced precursor cell differentiation and white to beige/brown adipocyte conversion (3). Furthermore, Gremlin 1 is a secreted protein, markedly increased in the adipose tissue in human hypertrophic obesity, while it is actually reduced in obese mice in which Noggin is primarily increased (3).

The increased levels of these antagonists in obese adipose tissue reduce BMP4 signaling, precursor cell commitment,

[1]Department of Molecular and Clinical Medicine, The Lundberg Laboratory for Diabetes Research, Sahlgrenska Academy, University of Gothenburg, Gothenburg, Sweden
[2]Wallenberg Centre for Molecular and Translational Medicine, University of Gothenburg, Gothenburg, Sweden
[3]Bioscience Metabolism, Research and Early Development, Cardiovascular, Renal and Metabolism (CVRM), BioPharmaceuticals R&D, AstraZeneca, Cambridge, U.K.
[4]Bioscience Metabolism, Research and Early Development, Cardiovascular, Renal and Metabolism (CVRM), BioPharmaceuticals R&D, AstraZeneca, Gothenburg, Sweden
[5]Department of Medicine, University of Leipzig, Leipzig, Germany

Corresponding author: Ulf Smith, ulf.smith@medic.gu.se

Received 16 July 2019 and accepted 8 December 2019

This article contains Supplementary Data online at https://diabetes.diabetesjournals.org/lookup/suppl/doi:10.2337/db19-0701/-/DC1.

and subsequent induction of beige/brown adipogenesis (1,3). Consistent with this, we have also demonstrated that BMP4 signaling is markedly reduced in the adipose tissue in obesity despite the increased expression and secretion of BMP4 (1,3). Taken together, these observations suggest that Gremlin 1 is an interesting target in human obesity and that it may also be involved in the development of hypertrophic obesity and the obese phenotype of insulin resistance complications (i.e., T2D and NAFLD/NASH), as a marker of increased ectopic fat accumulation. NAFLD is primary characterized by accumulation of intrahepatic triacylglycerols (TGs) and is present in 75–90% of subjects with T2D (6,7). NAFLD may progress to the severe condition of NASH, characterized by advanced histological remodeling including fibrosis, lobular inflammation, hepatocellular ballooning, and risk of liver cancer.

In this study, we measured Gremlin 1 serum levels and skeletal muscle, adipose tissue, and liver mRNA in cohorts without and with diabetes and in subjects with NAFLD/NASH. We also assessed the effect of Gremlin 1 on insulin signaling and action in these three major target tissues for insulin. Our results identify Gremlin 1 as a novel biomarker and potential therapeutic target in insulin resistance and associated complications.

RESEARCH DESIGN AND METHODS

Study Populations

All studies were performed in accordance with the Declaration of Helsinki. All subjects gave written informed consent before taking part in the studies.

Cohort FDR/Control

In this cohort, 34 nonobese subjects were studied: 17 individuals with at least one known first-degree relative (FDR) with T2D and 17 individuals without known genetic predisposition for T2D defined as no family history (control subjects). The groups were matched for sex (10 females in both groups) and BMI and had similar age (Table 1). Fasting plasma insulin and glucose levels were used to calculate insulin resistance defined as a HOMA of insulin resistance (HOMA-IR) index using the formula: HOMA-IR = (fasting plasma glucose × fasting plasma insulin)/22.5. Local subcutaneous adipose tissue biopsies were obtained from the lower abdominal wall as previously reported (3). Study protocol was approved (S655–03) by the Ethical Committee of the Sahlgrenska Academy, University of Gothenburg.

Other Cohorts

Paired samples of subcutaneous, omental visceral adipose tissue, and liver were collected during laparoscopic abdominal surgery as described previously (6). Adipose tissue was immediately frozen in liquid nitrogen and stored at −80°C. The study was approved by the Ethics Committee of the University of Leipzig (approval number 159–12–21052012; Leipzig, Germany). BMI was calculated by weight (kilograms) divided by square of height (meters).

- Cohort ND/D (Table 1): in a cross-sectional study, we investigated *GREMLIN 1* mRNA in paired visceral/omental and abdominal subcutaneous adipose tissue samples (n = 233; BMI >30 kg/m^2). Of these, 105 individuals had normal glucose levels, and 128 had T2D.
- Cohort GIR (Table 1): in 93 individuals (BMI 24–37 kg/m^2) with normal glucose tolerance (NGT), adipose tissue *GREMLIN 1* mRNA was evaluated in relation to the glucose infusion rate (GIR) in euglycemic-hyperinsulinemic clamps according to previously described procedures (6).
- Cohort ND/D/NAFLD (Table 1): a cohort of 52 obese individuals with wide range of liver fat content and with (n = 28; BMI 34 ± 5.8 kg/m^2) or without T2D (n = 23; BMI 34 ± 5.9 kg/m^2) were studied. *GREMLIN 1* mRNA was measured both in paired adipose tissue and liver samples. For measurement of metabolic parameters, all baseline blood samples were collected between 8 and 10 A.M. after an overnight fast and analyzed as previously described (6).
- Cohort Nob/obND/obD (Table 1): serum Gremlin 1 levels were analyzed in 45 individuals with either NGT (n = 30)

Table 1—Cohort data

Cohort FDR/control	
n (total)	34
n (FDR)	17
n (control)	17
BMI, kg/m^2	24 ± 1.3
Age, years	35.9 ± 8.5
Cohort ND/D	
n (total)	233
n (T2D)	128
n (NGT)	105
BMI, kg/m^2	50.6 ± 14
Age, years	45.1 ± 13.2
Cohort GIR	
N (total)	93
BMI, kg/m^2	31.1 ± 5.9
Age, years	57.1 ± 15
Cohort ND/D/NAFLD	
n (total)	51
n (T2D)	23
n (NGT)	24
BMI, kg/m^2	34 ± 5.8
Age, years	66 ± 12.3
Cohort Nob/obND/obD	
n (total)	45
Lean BMI, kg/m^2	22 ± 2.4
Obese NGT BMI, kg/m^2	45.4 ± 6.2
Obese T2D BMI, kg/m^2	46.2 ± 5.7
Age, years	66 ± 12.3
CRP, mg/L	4.5 ± 3.5
ALAT, μkat/L	0.4 ± 0.2
ASAT, μkat/L	0.4 ± 0.1
HOMA-IR	7 ± 8
HbA_{1c}, %	6.2 ± 1.7
Cohort two-step bariatric surgery intervention	
n (total)	55

Data are mean ± SD unless otherwise indicated.

with a BMI <25 kg/m^2 ($n = 15$) or >30 kg/m^2 ($n = 15$) or with known T2D ($n = 15$).
- Two-step bariatric surgery intervention was a cohort of 55 individuals with morbid obesity who underwent a two-step bariatric surgery approach with a sleeve gastrectomy as a first step and, after 12 ± 2 months, a Roux-en-Y gastric bypass surgery as the second step as previously reported (8).

These different cohorts were also essentially sex neutral, with ~70% females and 30% males, and are summarized as a flow chart in Supplementary Fig. 1.

Diagnosis of Diabetes

The diagnosis of T2D versus normal or impaired glucose tolerance was based on the results of a 75-g oral glucose tolerance test according to the criteria of the American Diabetes Association (9). T2D was defined by 120-min glucose ≥11.1 mmol/L or a repeated fasting plasma glucose ≥7.0 mmol/L.

Virtually all of the patients with diabetes were treated with metformin and some, as needed, with a dipeptidyl peptidase inhibitor. Only these medications were used for diabetes treatment in these cohorts. Patients with elevated cholesterol and/or blood pressure received regular medication as required.

Diagnosis of NAFLD/NASH

In the human cohort for which parallel liver and adipose tissue biopsies were available, NAFLD and NASH have been determined and diagnosed histologically (using hematoxylin and eosin–stained and Masson trichrome–stained slides) following a previous proposal for grading and staging of the histological lesions detected in liver biopsies (10). In accordance, two independent and specialized liver pathologists at the University of Leipzig evaluated the histological lesions—steatosis, ballooning, and intra-acinar and portal inflammation—and summarized those in the score (11).

Detection of Gremlin 1 in Human Serum

Sandwich ELISA was used to measure human serum Gremlin 1 levels in the samples. Gremlin 1 was captured using an in-house–developed monoclonal antibody against Gremlin 1 (MedImmune, Gaithersburg, MD) on a 96-well half-area plate. The samples were incubated for 1 to 2 h followed by detection with rabbit polyclonal antibody (catalog number ab157576; Abcam) for 1 h. The rabbit polyclonal was detected using in-house–generated horseradish peroxidase–conjugated anti-rabbit polyclonal antibody. Gremlin 1 levels in the samples were interpolated using the standard curve generated in 50% immune-depleted serum.

Cell-Based Experiments

Primary Human Adipocytes

Primary human adipocytes were isolated as previously described (12). Briefly, subcutaneous adipose tissues, obtained by needle biopsy, were digested with collagenase type II (Sigma-Aldrich, St. Louis, MO) for 60 min at 37°C in shaking water bath. The adipocytes were then filtered through a 250-μm nylon mesh and washed four times, followed by cell size measurement, RNA/protein extractions, and/or additional experimental assays. For insulin signaling and glucose uptake assessments, adipocytes were further incubated in Hank's medium 199, pH 7.4 (Life Technologies, Carlsbad, CA) containing 4% BSA with or without 6 mmol/L glucose, respectively.

For glucose uptake, the adipocytes were pretreated with IgG or anti–Gremlin 1 antibody (MedImmune) and/or recombinant Gremlin 1 (200 ng/mL) (R&D Systems, Inc., Minneapolis, MN) for 3 h and stimulated with 10 nmol/L insulin for 15 min before the addition of D-[U-^{14}C] glucose (0.26 mCi/L; final concentration 0.86 μmol/L) (PerkinElmer, Waltham, MA) for additional 45 min. The glucose uptake was immediately stopped by separating the adipocytes from the medium, and incorporated radioactivity was measured in a scintillation counter.

Primary Skeletal Muscle Cells

Satellite cells were isolated from five donors with NGT. The cells were grown to >80% confluence in DMEM/F12 containing 10% FBS and antibiotics and further differentiated into multinuclear myotubes in differentiation medium (DMEM, Medium 199, HEPES, zinc sulfate, vitamin B12, FBS, and antibiotics) as described (13). Cells were then starved for 4 h before incubation with recombinant Gremlin 1 (50 ng/mL) and insulin (1–10 nmol/L).

Human Hepatocytes

Primary human hepatocytes, HiPS-Hep (Takara Bio Inc., Shiga, Japan), were cultured in hepatocyte medium (Takara Bio) according to the manufacturer's instructions. Cells were starved 3 h before pretreatment with recombinant Gremlin 1 (50 ng/mL) and insulin (100 nmol/L).

HepG2 liver cells (ATCC, Manassas, VA) and IHH (human hepatocyte celline) were cultured in DMEM (Lonza, Basel, Switzerland) supplemented with 10% FBS and antibiotics. To study the secretory effects of Gremlin 1, HepG2 cells were transfected with wt.Grem1.myc or trunc.Grem1.myc plasmids (expressing myc-tag fused to the COOH-terminal of human Gremlin 1 with or without the N-terminal signal peptide sequence) constructed in our laboratory. For confocal imaging, the cells were grown on glass chamber slides (Thermo Fisher Scientific) for 72 h. Cells were then washed with PBS, fixed with 4% formaldehyde, permeabilized with 0.1% Triton, blocked by 20% goat serum (1 h), and incubated with anti–myc antibody (Sigma-Aldrich) for 3 h. After washing with PBS and incubation with Alexa 488–probed secondary antibody for 1 h, cells were mounted with Vectashield mounting solution containing DAPI (Vector Laboratories, Inc). Confocal images were then collected with the Leica SP5 confocal microscope.

To study the effect of protein tyrosine phosphatase 1B (PTP1B) inhibitor (CAS 765317–72–4; Merck Millipore, Danvers, MA), IHHs were starved and pretreated with the inhibitor (10 μmol/L) with or without recombinant Gremlin 1 (200 ng/mL) for 24 h, followed by insulin (10 nmol/L) for 10 min.

Quantitative Real-time PCR

mRNA was extracted from cells and tissues followed by cDNA synthesis. The gene expression was then analyzed using the QuantStudio 6 Flex TaqMan system (Applied Biosystems, Foster City, CA). Relative quantification of gene expression was normalized to 18S rRNA or HPRT1. The primers and probes were either designed or ordered commercially as predesigned TaqMan probe kits (Assay On-Demand; Applied Biosystems).

Immunoblotting

Western blot analysis were performed as previously described (14). The following primary antibodies were used: Gremlin 1 (MedImmune), pAktS473, AKT (Cell Signaling Technology, Danvers, MA), pY20, IRβ (Santa Cruz Biotechnology, Dallas, TX), and IRS1 (Merck Millipore).

PTP1B Activity Assay

PTP1B activity was assessed using the PTP activity assay kit (Millipore). Briefly, IHHs were lysed in lysis buffer lacking sodium orthovanadate. PTP1B was then immonoprecipitated using a PTP1B antibody (Millipore). The measurement of PTP1B activity was carried out using the synthetic Tyrosine Phosphopeptide (TSTEPQpYQPGENL). The phosphate release was measured at OD 650 nmol/L using the malachite green reagent provided with the kit.

Statistical Analysis

The experimental data are shown as means ± SD or means ± SEM. Significance is indicated in the figures as $P < 0.05$, $P < 0.01$, and $P < 0.001$. All statistical calculations were performed using IBM SPSS Statistics v20. Pairwise comparisons were performed using the Student *t* test. For multiple comparisons, one-way ANOVA with Bonferoni post hoc test or Kruskal-Wallis test was used when appropriate. To assess correlation between variables, Pearson or Spearman correlations were used as appropriate. Statistical analysis of the cohorts did not differentiate between females and males because they were all characterized by ~70% females and 30% males.

Data and Resource Availability

The data set and resources generated and analyzed in this study are available from the corresponding author upon reasonable request. The suppliers of antibodies used in this study have been cited above.

RESULTS

Increased Gremlin 1 in Adipose Tissue, Liver, and Serum in Insulin Resistance and T2D Independent of BMI

To identify if transcriptional activation of Gremlin 1 is altered in insulin resistance, obesity, T2D, and NAFLD/NASH, we examined tissue mRNA in five different cohorts. In the cohort consisting of sex-, BMI-, and age-matched nonobese control subjects (BMI 24.3 ± 2.4 kg/m^2, age 34 ± 9 years) and FDRs (BMI 24.9 ± 2.3 kg/m^2, age 38 ± 8 years) of subjects with T2D, *GREMLIN 1* mRNA was significantly higher in the subcutaneous adipose tissue of this high-risk FDR subgroup compared with the matched control group (Fig. 1*A*). In addition, *GREMLIN 1* levels were positively correlated with percentage of body fat and insulin resistance measured as HOMA-IR (Fig. 1*B* and *C*). FDRs as a group are more insulin resistant than a BMI-matched non-FDR group.

In the cohorts consisting of subgroups without diabetes and with T2D (ND/D and ND/D/NAFLD cohorts), *GREMLIN 1* mRNA was higher in visceral than in subcutaneous adipose tissue in both ND/D subgroups and increased in both tissues in T2D compared with individuals with NGT (Fig. 1*D* and *F*). Moreover, *GREMLIN 1* mRNA levels in both visceral and subcutaneous adipose tissue were again negatively correlated with insulin sensitivity in individuals without diabetes (cohort GIR), measured by hyperinsulinemic-euglycemic clamps (Fig. 1*E* in visceral and Supplementary Fig. 2*A* in subcutaneous adipose tissue). We also found hepatic *GREMLIN 1* mRNA to be increased in patients with T2D of the ND/D/NAFLD cohort (Fig. 1*G*). There was no correlation between age and *GREMLIN 1* mRNA levels in either subcutaneous or visceral adipose tissue in the large ND/D cohort of 216 individuals.

As Gremlin 1 is a secreted protein, we asked if its circulating levels are altered in insulin resistance and T2D. Current ELISAs and commercially available antibodies are not very sensitive, so we used the modified in-house ELISA with a noncommercially available antibody as described (3). We analyzed high-quality serum from the Nob/obND/obD cohorts consisting of nonobese NGT, obese NGT, and equally obese subjects with T2D. Serum Gremlin 1 tended to be higher in the obese than in the nonobese subjects, but it was further significantly increased in equally obese individuals with T2D (Fig. 1*H*). This observation is consistent with our results of increased adipose tissue and liver *GREMLIN 1* mRNA expression in patients with T2D. In addition, circulating levels of Gremlin 1 were positively and significantly correlated with HOMA-IR (Fig. 1*I*) as well as with glycosylated hemoglobin (HbA_{1c}) (Fig. 1*J*). Collectively, these results provide evidence that *GREMLIN 1* mRNA levels in adipose tissue and liver as well as circulating serum levels are associated with both degree of insulin resistance and obesity and also increased in established T2D irrespective of degree of obesity. However, in contrast to adipose tissue and liver *GREMLIN 1*, skeletal muscle expression was not increased in biopsies from individuals with T2D compared with individuals without diabetes (data not shown).

Secreted Gremlin 1 Impairs Insulin Signaling and Action in Adipose, Skeletal Muscle, and Liver Cells but Not Through PTP1B Activation

Because both adipose tissue and liver *GREMLIN 1* mRNA and serum Gremlin 1 levels were strongly associated with degree of insulin resistance and its associated consequences, we assessed the possible effect of Gremlin 1 on insulin signaling in key human target cells.

We characterized the direct effect of Gremlin 1 protein on insulin signaling in human primary adipocytes, human

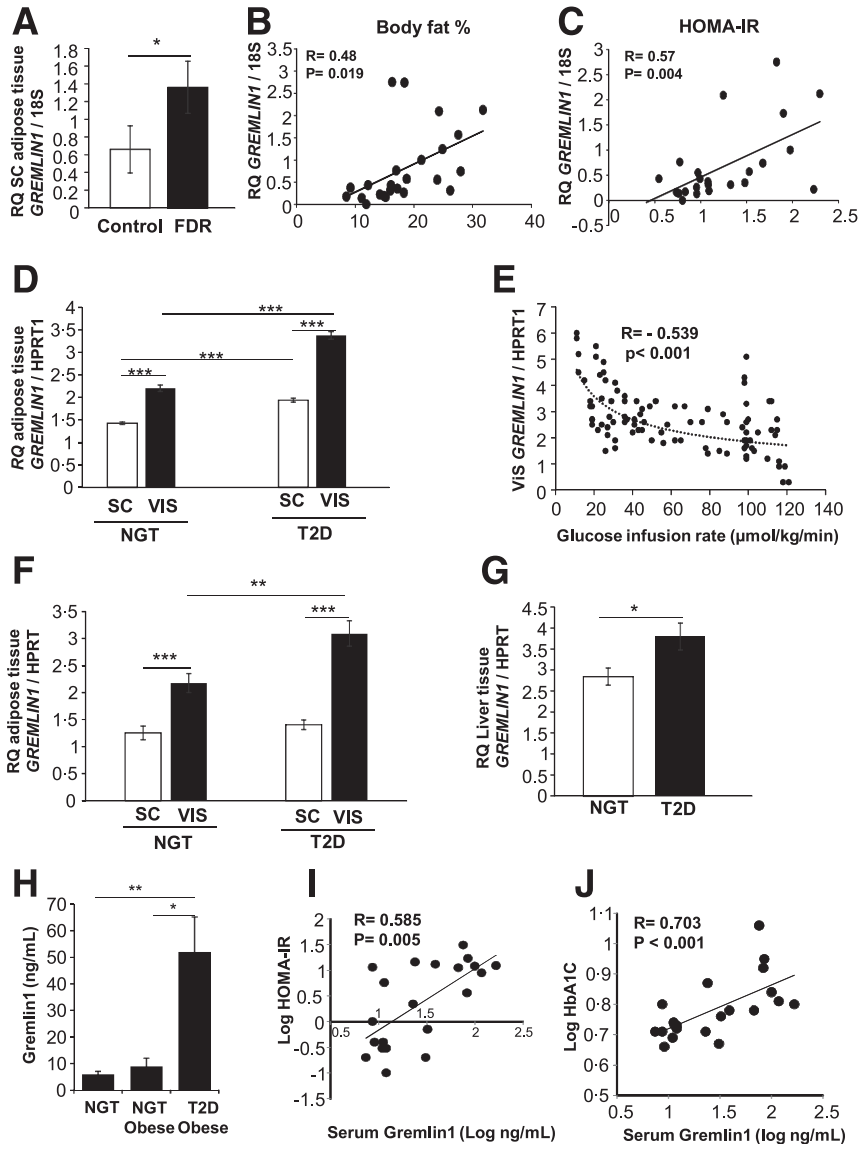

Figure 1—*GREMLIN 1* mRNA in adipose tissue and liver and circulating levels of Gremlin 1 are increased in insulin resistance and T2D. *A*: Differential *GREMLIN 1* mRNA in subcutaneous (SC) adipose tissue in individuals with genetic predisposition for T2D (FDR) and matched control subjects in FDR/control cohort. Correlation to body fat percentage (*B*) and HOMA-IR (*C*) in the same cohort. *D*: *GREMLIN 1* mRNA in SC and visceral (VIS) adipose tissue in individuals with T2D and with NGT in ND/D cohort. *E*: *GREMLIN 1* mRNA in VIS adipose tissue is inversely correlated to GIR during hyperinsulinemic-euglycemic clamps in cohort GIR. *GREMLIN 1* mRNA expression in adipose tissue (*F*) and liver (*G*) in individuals with T2D and with NGT in ND/D/NAFLD cohort. Circulating levels of Gremlin 1 in lean NGT, obese NGT, and equally obese subjects with T2D in cohort Nob/NDob/obD (*H*) and relation to HOMA-IR (*I*) and HbA_{1c} (*J*). All graphs display means ± SEM. Statistics were calculated using Mann-Whitney test (*A*), Kruskal-Wallis one-way analysis (*D* and *H*), and ANOVA with Bonferoni post hoc test (*F* and *G*). $^{*}P < 0.05$; $^{**}P < 0.01$; $^{***}P < 0.001$. RQ, relative quantification.

induced pluripotent stem cell–derived hepatocytes, HepG2, IHHs, and primary human differentiated skeletal muscle cells. Short-term incubations (2–4 h) with recombinant human Gremlin 1 significantly impaired insulin signaling measured as phosphorylation of pS473-AKT in all human cells. We also examined the effect on tyrosine phosphorylation in human adipose cells, and the pY-IRβ subunit was also reduced (Fig. 2*A*–*C*). We further examined the effect of Gremlin 1 protein on both basal and insulin-stimulated glucose uptake in adipocytes isolated from subcutaneous adipose tissue biopsies of 11 subjects (BMI 22–37 kg/m^2). Recombinant Gremlin 1 significantly reduced glucose uptake in response to insulin, and this effect was neutralized by anti–Gremlin 1 antibody (Fig. 2*D*). In fact, the addition of anti–Gremlin 1 alone significantly improved insulin-stimulated glucose uptake, and this sensitizing effect was related to the initial insulin response (i.e., the lower the incremental insulin response, the larger the positive effect of anti–Gremlin 1 alone on insulin-stimulated glucose uptake) (Fig. 2*E*). This was further validated by the positive correlation

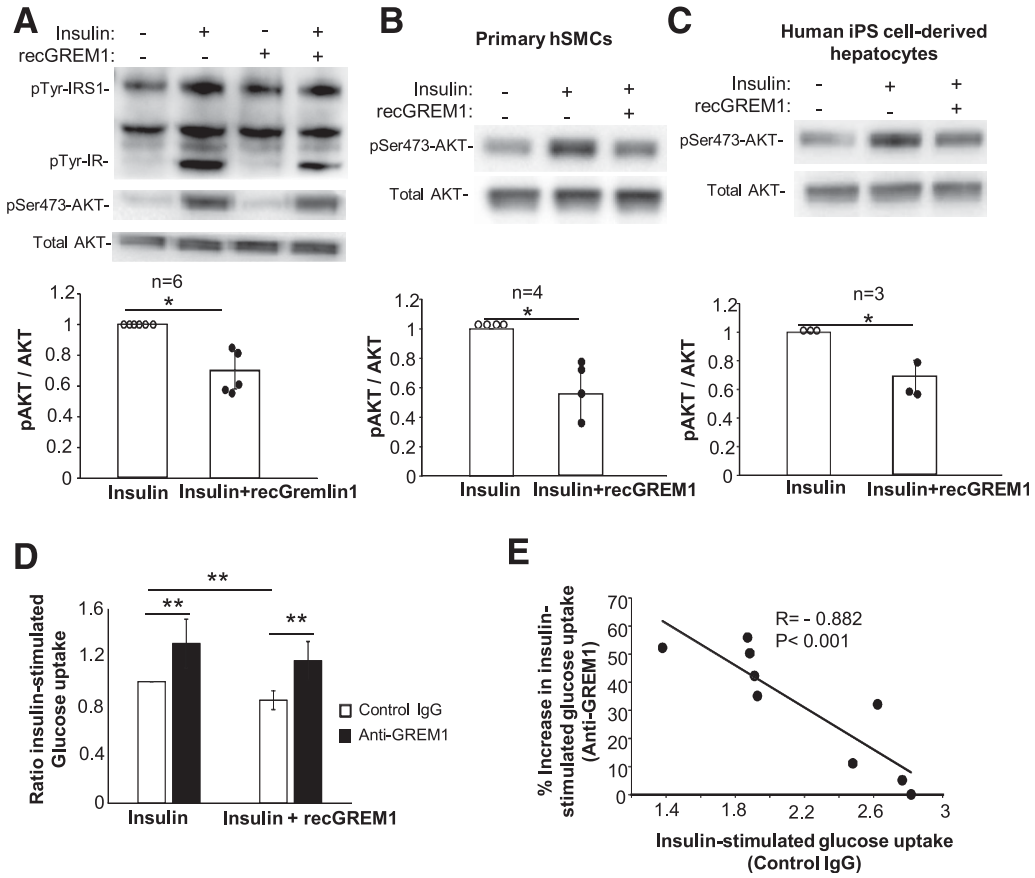

Figure 2—Gremlin 1 inhibits insulin signaling and action. Representative immunoblot analysis with quantifications showing that incubation with recombinant Gremlin 1 (recGREM1) inhibits insulin-induced tyrosine phospho–insulin receptor (pTyr-IR) (*A*) and serine 473 phospho-AKT (pSer473-AKT) in isolated primary human adipocytes ($n = 6$) and in primary human differentiated skeletal muscle cells (hSMCs) ($n = 4$) (*B*) and human induced pluripotent stem cell (iPS)-derived hepatocytes ($n = 3$) (*C*). *D*: Incubation with recGREM1 decreased insulin-stimulated glucose uptake in isolated primary human adipocytes ($n = 11$). Presence of anti–Gremlin 1 increased insulin-stimulated glucose uptake and antagonized the effect of recGREM1 compared with adipocytes treated with control IgG ($n = 9$). *E*: Correlation between the increase in insulin-stimulated glucose uptake in adipocytes treated with anti–Gremlin 1 antibody and the degree of initial insulin glucose uptake in same cells treated with control IgG. Graphs display means ± SD. Statistics were calculated using the Student *t* test (*A–C*) and ANOVA with Bonferoni post hoc test (*D*). $^*P < 0.05$; $^{**}P < 0.01$.

between HOMA-IR, as a marker of donor insulin sensitivity, and the incremental effect of the anti–Gremlin 1 antibody (Supplementary Fig. 3*A*). These data suggest that Gremlin 1 secretion by adipose cells, which we have also previously demonstrated (3), is directly antagonistic to the effect of insulin and contributing to insulin resistance in the cells. If the effect on glucose uptake is also secondary to the insulin-antagonizing effect or indicates additional effects of Gremlin 1 on GLUT4 protein recycling remains to be studied.

To further verify the insulin-antagonistic effect of Gremlin 1 as a secreted molecule, we expressed a nonsecreted truncated and a secreted full-length Gremlin 1 in human HepG2 hepatocytes. We found that only the secreted, and not the nonsecreted, form inhibited insulin signaling (Fig. 3*A*). This inhibitory effect of secreted Gremlin 1 was again prevented by anti–Gremlin 1 antibody (Supplementary Fig. 2*B*). Additionally, full-length Gremlin 1 was primarily localized in the cytoplasm prior to its secretion, while the truncated form was only detected in the cell nuclei (Fig. 3*B*). Nuclear localization of Gremlin 1 has previously been reported by several studies suggesting other functional roles for the nuclear Gremlin 1 (12).

PTP1B is a well-known inhibitor of insulin signaling and has been a potential therapeutic target for treating T2D (15,16). Considering the reduced tyrosine phosphorylation of the insulin receptor, we asked if Gremlin 1 interferes with PTP1B signaling. IHHs were incubated with a PTP1B inhibitor and/or recombinant Gremlin 1 followed by insulin stimulation. The inhibition of PTP1B by its inhibitor enhanced insulin signaling as expected, and this was seen whether or not Gremlin 1 was present (Fig. 4*A*). Furthermore, we did not see any direct effect of Gremlin 1 on PTP1B activity (Fig. 4*B*). Thus, these data do not support that the inhibitory effect of Gremlin 1 on insulin signaling is due to increased PTPB1 activity.

In sum, these data show that secreted and circulating Gremlin 1, probably emanating from the adipose tissue to a large extent in vivo, is insulin antagonistic in all three

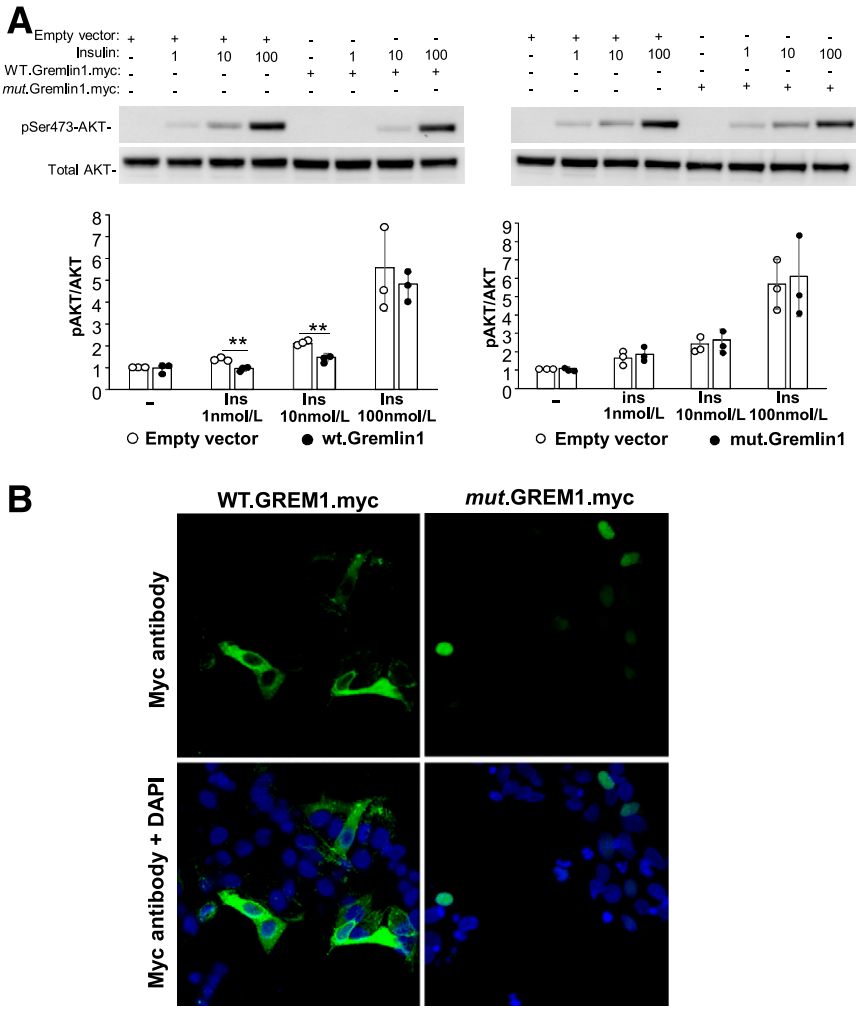

Figure 3—Insulin signaling is inhibited by secreted Gremlin 1 and not a truncated nonsecreted form of Gremlin 1. *A*: Representative immunoblot analysis showing that insulin-stimulated serine 473 phospho-AKT (pSer473-AKT) is inhibited in HepG2 hepatocytes transfected with wild-type Gremlin 1 (WT.GREM1.myc) but not in cells transfected with a truncated Gremlin 1 that is not secreted (*mut*.GREM1.myc) ($n = 3$). *B*: Cellular localization of WT.GREM1.myc and *mut*.GREM1.myc in HepG2 hepatocytes stained by Myc antibody (green) and DAPI (blue) and imaged with a confocal microscope. $^{**}P < 0.01$.

major human target cells. However, the mechanisms for this inhibitory effect are currently unclear.

To further validate the adipose tissue as an important source of serum Gremlin 1 levels, we investigated if circulating Gremlin 1 was related to serum adiponectin levels and found a significant negative correlation ($R = -0.28$; $P < 0.01$). Negative correlations with adiponectin levels were also seen with adipose tissue *GREMLIN 1* mRNA levels in cohort ND/D (subcutaneous tissue, $R = -0.23$, $P < 0.01$; visceral tissue, $R = -0.35$, $P < 0.001$) and in cohort ND/D/NAFLD (subcutaneous tissue, $R = -0.24$, $P < 0.05$; visceral tissue, $R = -0.31$, $P < 0.05$).

The importance of the adipose tissue as a source for Gremlin 1 was further documented in the bariatric surgery investigation cohort of 55 individuals with obesity who underwent the two-step bariatric surgery approach, losing ~50 kg body weight. *GREMLIN 1* mRNA expression, both in subcutaneous and visceral adipose tissues, was significantly reduced (Supplementary Fig. 3*B*). Thus, the increased Gremlin 1 levels in obesity and T2D are likely to be associated with the increased adipose tissue.

Increased Adipose Tissue, Liver, and Serum Gremlin 1 Levels Are Associated With Markers of NAFLD/NASH

As tissue Gremlin 1 expression and function are associated with obesity and insulin resistance/T2D, we next examined if it also was related to other insulin resistance/obesity-linked complications such as NAFLD/NASH. To accomplish this, liver biopsies from 52 obese individuals with or without T2D (cohort ND/D/NAFLD) were carefully characterized using the NAFLD/NASH scoring system as defined by international guidelines (17).

We found transcriptional activation of *GREMLIN 1* in the subcutaneous and visceral adipose tissue and the liver

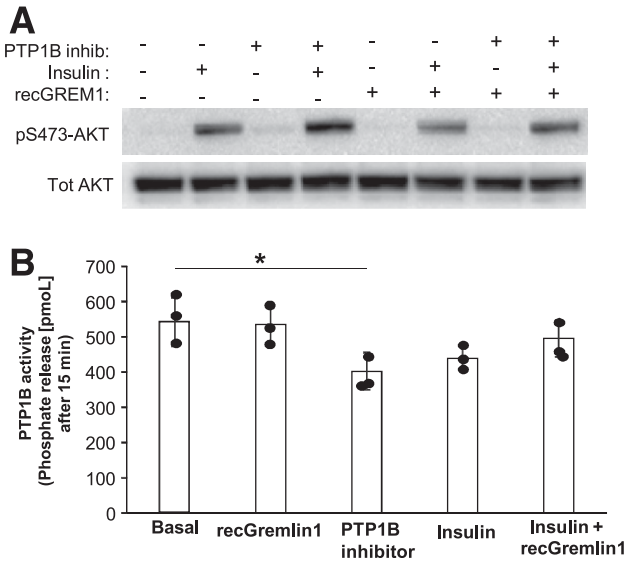

Figure 4—Gremlin 1 and PTP1B activity. *A*: Representative immunoblot analysis showing that inhibition of PTP1B (PTP1B inhib) increases insulin-stimulated AKT phosphorylation and reverses the effect of recombinant Gremlin 1 (recGREM1) in IHHs ($n = 4$). *B*: PTP1B activity in IHHs treated with recGremlin 1, PTP1B inhibitor, or insulin. Graphs display means ± SD. Statistics were calculated using Student *t* test. *$P < 0.05$. Tot, total.

Table 2—Levels of *GREMLIN 1* in visceral and subcutaneous adipose tissue and liver (cohort ND/D/NAFLD)

	VIS *GREMLIN 1*	SC *GREMLIN 1*	Liver *GREMLIN 1*
Serum adiponectin, ng/mL (4.5 ± 2.5)	−0.31*	−0.24*	−0.31*
Liver fat, % (20.8 ± 13)	0.48***	0.40**	0.25*
Serum FFA, mmol/L (0.6 ± 0.3)	0.37**	0.40**	0.26*
Serum TG, mmol/L (184 ± 60.5)	0.37**	0.29*	0.46**
Serum LDL-C, mmol/L (4.7 ± 1.6)	0.23 ($P = 0.065$)	0.28*	0.17
Serum IL-6, pmol/L (3.9 ± 2.8)	0.41**	0.20	0.32**
Fasting serum insulin, pmol/L (204 ± 136)	0.39**	0.42**	0.40**
NASH score steatosis	0.24 ($P = 0.099$)	0.25 ($P = 0.075$)	0.41**
NASH score ballooning	0.25 ($P = 0.075$)	0.34*	0.52**
NASH score inflammation	0.11	0.32*	0.33*
NASH score fibrosis	0.24 ($P = 0.098$)	0.22	0.39**

Data are *R* values or mean ± SD. FFA, free fatty acid; IL-6, interleukin-6; LDL-C, LDL cholesterol; SC, subcutaneous adipose tissue; VIS, visceral adipose tissue. *$P < 0.05$; **$P < 0.01$; ***$P < 0.001$.

to be positively associated with NAFLD activity scores, including degree of steatosis, ballooning, as well as inflammation and fibrosis scores (Table 2). In addition, they were negatively associated with other markers of insulin sensitivity, including serum adiponectin levels, and positively with liver fat content, circulating free fatty acids, TGs, low HDL cholesterol, and the cytokine interleukin-6 (i.e., key markers of the metabolic syndrome) (Table 2). Of interest, we also observed significantly higher liver *GREMLIN 1* mRNA in patients with T2D with biopsy-proven NASH compared with patients with T2D with only NAFLD. This increase was not seen in the NGT individuals (Fig. 5*A*).

Consistent with these findings, we found circulating levels of Gremlin 1 (Nob/obND/obD) to be significantly, and positively, correlated with serum levels of C-reactive protein (CRP), alanine aminotransferase (ALAT), and aspartate aminotransferase (ASAT), which are all markers of NALFD/NASH (Fig. 5*B–D*).

Taken together, these data show that Gremlin 1 is a secreted and insulin-antagonistic protein, particularly highly expressed in the visceral adipose tissue, increased in both adipose tissue and liver in obesity and T2D, and related to the degree of whole-body insulin resistance and NAFLD/NASH. These novel findings make Gremlin 1 an interesting potential therapeutic target in obesity and insulin resistance, T2D, and NAFLD/NASH.

DISCUSSION

BMP4 is a critical regulator of human adipose precursor cell commitment and differentiation (reviewed in Hoffmann et al. [1]), and maintained BMP signaling promotes browning of the differentiated white adipose cells in both murine models and human cells (1,2,5), while brown adipose cells become beige and less oxidative (1,5). Because Gremlin 1 is a secreted protein by human adipose cells and a key endogenous regulator of BMP signaling in these cells (3), we wanted to examine its presence in other metabolic tissues and the relation to obesity and its complications.

In this study, we investigated in several well-characterized large cohorts if Gremlin 1 serum levels and transcriptional activation in the subcutaneous and visceral adipose tissue, liver, and skeletal muscle also are related to the obesity phenotype and associated complications of T2D and NAFLD/NASH. We show that *GREMLIN 1* mRNA levels are particularly high in visceral, compared with subcutaneous, adipose tissue and that insulin sensitivity measured with both euglycemic clamps and the clinical HOMA index showed strong negative correlations between adipose tissue expression in both regions and insulin sensitivity. This is consistent with our previous finding that Gremlin 1 is a secreted protein and markedly increased in subcutaneous adipose tissue with expanded adipose cells (3) (i.e., in hypertrophic obesity), which is related to insulin resistance and other obesity-associated complications (reviewed in Hoffmann et al. [1]). Because we previously found Gremlin 1 to antagonize the

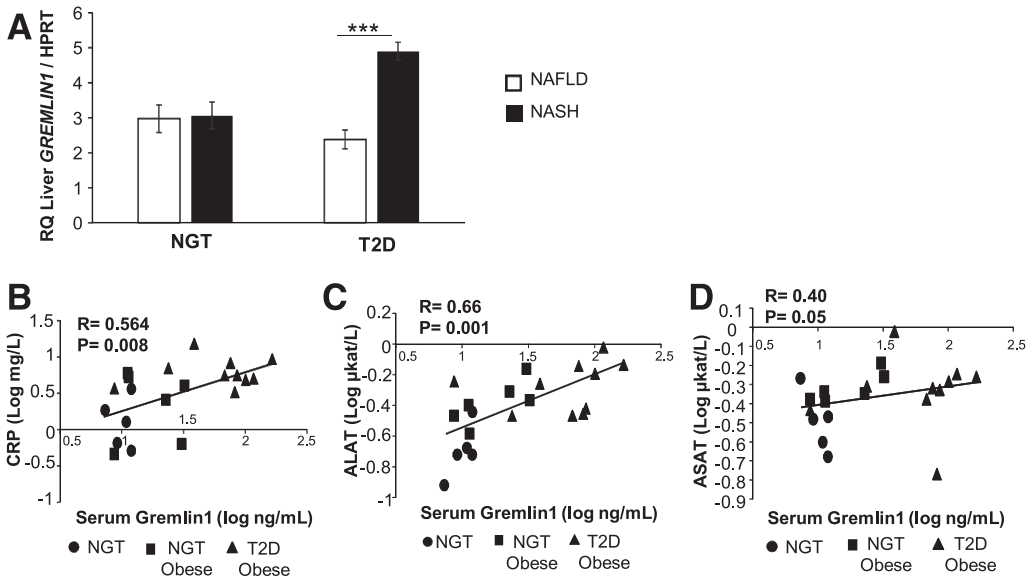

Figure 5—Gremlin 1 levels and NAFLD/NASH. *A*: *GREMLIN 1* mRNA in liver biopsies of individuals with NAFLD or NASH and in individuals with or without T2D in cohort ND/D/NAFLD. Circulating levels of Gremlin 1 correlate with CRP (*B*), ALAT (*C*), and ASAT (*D*). Graphs display means ± SEM. Statistics were calculated using Student *t* test. ***$P < 0.001$. RQ, relative quantification.

early induction of adipogenesis, it is not unexpected that it is also increased in the adipose tissue in hypertrophic, insulin-resistant obesity. Although our current data cannot prove causality in terms of increased adipose tissue Gremlin 1 directly leading to the development of hypertrophic, insulin-resistant obesity, we also cannot exclude it. Apart from our previous experimental studies (3), additional support for this possibility is our current finding that *GREMLIN 1* mRNA levels also were increased in lean and fairly young FDR individuals. FDRs are characterized by insulin resistance, an impaired subcutaneous adipogenesis, and development of inappropriately expanded adipose cells (i.e., hypertrophic obesity) (18,19). In addition, recent large studies have demonstrated that individuals with genetic markers of insulin resistance are characterized by reduced subcutaneous adipose tissue, which, even if cell size was not measured, implies an association with impaired adipogenesis (20).

We have tried to investigate the effects of increased Gremlin 1 serum levels in a murine in vivo model by expressing it in the liver of mature mice with AAV8–Gremlin 1 (R.K.S., J.M. Hoffmann, S.H., S. Heasman, C.C., I. Elias, F. Bosch, J.B., A.H., U.S., unpublished observations). However, mature mouse models are not responsive to increased Gremlin 1 targeting the liver with gene therapy because it accumulated in the liver cells and was apparently not secreted. Also, we did not see any increase in liver inflammation or fibrosis in this model. In addition, intraperitoneal injections were essentially without any effects on phenotype, and Gremlin 1 protein did not antagonize the effect of insulin in murine cells like those that we find in this study in human cells. Thus, mature mice are not good models to characterize effects of Gremlin 1 in vivo.

Consistent with our current in vivo findings of increased Gremlin 1 levels in insulin resistance, we also find Gremlin 1 protein to directly antagonize insulin signaling in three key target cells for insulin. The inhibitory effect of recombinant and cell-secreted Gremlin 1 and the sensitizing effect of anti–Gremlin 1 on insulin-induced glucose uptake show that Gremlin 1 can attenuate both insulin signaling and insulin-stimulated glucose transport, although these may be partly linked. We also found that the insulin-sensitizing effect of anti–Gremlin 1 is related to degree of cellular insulin responsiveness. Thus, the efficacy of anti–Gremlin 1 treatment is more pronounced in insulin-resistant cells, supporting a direct "tonic" inhibitory effect of Gremlin 1 secreted by the adipose cells. This concept is also supported by our finding of a positive correlation between the magnitude of the insulin-sensitizing effect of anti–Gremlin 1 and HOMA-IR (Supplementary Fig. 3*A*). *GREMLIN 1* mRNA levels were similar in both adipose tissue and liver, but considering the large adipose depot, it is probably a major source of circulating Gremlin 1. This is supported by the reduced *GREMLIN 1* levels in the adipose tissue after substantial weight reduction with bariatric surgery. Furthermore, *GREMLIN 1* was particularly high in visceral adipose tissue, which is drained by the portal circulation, thus targeting the liver with consequences for insulin resistance and other factors enhancing NAFLD/NASH development. Expanded visceral adipose depot is associated with insulin resistance and exhibits strong associations with future risk of developing cardiometabolic complications (6,21,22).

We also aimed at identifying mechanisms underlying the insulin-antagonistic effect of Gremlin 1. PTP1B, which is a key phosphatase and inhibitor of insulin signaling, has been extensively studied in vitro and in vivo and is considered as a potential therapeutic target for T2D (23–25). Although inhibiting PTP1B nonspecifically reduced the antagonizing

effect of Gremlin 1 on insulin signaling, PTP1B activity was not increased in Gremlin 1–treated cells. Thus, our data do not provide any support for PTP1B as a mediator of the reduced insulin signaling by Gremlin 1.

Gremlin 1 is a member of the DAN family of protein antagonists, primarily inhibiting BMP2 and BMP4, but has also been found to have other non-BMP binding partners such as the Slit protein in monocytes and, unexpectedly, also vascular endothelial growth factor receptor 2 with effects on angiogenesis (26). However, vascular endothelial growth factor receptor 2 as a binding partner could not be confirmed in a recent extensive study (27). It is also unlikely that the inhibitory effects of Gremlin 1 on insulin signaling, which are seen very rapidly (within a few hours), can be accounted for by its inhibitory effects on adipogenesis. This effect of Gremlin 1 is primarily due to inhibiting the early adipogenic commitment effects of BMP4 on the progenitor cells (3). However, direct or indirect effects of cell-endogenous or -exogenous circulating BMP4 on cellular insulin signaling and action cannot be excluded. In our previous study in mice treated with BMP4 gene therapy targeting the liver to increase circulating BMP4 levels, we found increased whole-body insulin sensitivity independent of any change in body weight (1). This has been further examined with similar positive effects on insulin sensitivity in obese mice (28). Thus, we currently favor the concept that Gremlin 1 inhibits insulin signaling and action by antagonizing the positive effects of BMP4, but this needs to be further substantiated.

In summary, our results identify Gremlin 1 as a prominent adipokine and cell-secreted antagonist of insulin signaling in human adipocytes, skeletal muscle cells, and liver cells. We also found Gremlin 1 serum and tissue levels to be significantly increased in insulin resistance and in individuals with T2D and NAFLD/NASH independent of degree of obesity. Thus, Gremlin 1 is an attractive novel therapeutic target in insulin resistance and associated complications of T2D and NAFLD/NASH.

Acknowledgments. The authors thank Dr. Ruchi Gupta (MedImmune, Gaithersburg, MD) for developing the serum Gremlin 1 ELISA technique.

Funding. Financial support for these studies was provided by the Medical Research Council, the Novo Nordisk Foundation, Torsten Söderberg Foundation, Swedish Diabetes Foundation, Swedish Agreement on Medical Education and Research contribution, and MedImmune (Gaithersburg, MD).

Duality of Interest. No potential conflicts of interest relevant to this article were reported.

Author Contributions. S.H., A.H., M.B., and U.S. designed the studies. S.H., R.K.S., A.H., L.B., and M.B. performed experiments. S.H. and U.S. wrote the paper with input from all authors. All authors have approved the manuscript. U.S. is the guarantor of this work and, as such, had full access to all of the data in the study and takes responsibility for the integrity of the data and the accuracy of the data analysis.

References

1. Hoffmann JM, Grünberg JR, Church C, et al. BMP4 gene therapy in mature mice reduces BAT activation but protects from obesity by browning subcutaneous adipose tissue. Cell Rep 2017;20:1038–1049

2. Qian S-W, Tang Y, Li X, et al. BMP4-mediated brown fat-like changes in white adipose tissue alter glucose and energy homeostasis. Proc Natl Acad Sci U S A 2013;110:E798–E807

3. Gustafson B, Hammarstedt A, Hedjazifar S, et al. BMP4 and BMP antagonists regulate human white and beige adipogenesis. Diabetes 2015;64:1670–1681

4. Hammarstedt A, Gogg S, Hedjazifar S, Nerstedt A, Smith U. Impaired adipogenesis and dysfunctional adipose tissue in human hypertrophic obesity. Physiol Rev 2018;98:1911–1941

5. Modica S, Straub LG, Balaz M, et al. Bmp4 promotes a brown to white-like adipocyte shift. Cell Rep 2016;16:2243–2258

6. Klöting N, Fasshauer M, Dietrich A, et al. Insulin-sensitive obesity. Am J Physiol Endocrinol Metab 2010;299:E506–E515

7. Younossi ZM, Koenig AB, Abdelatif D, Fazel Y, Henry L, Wymer M. Global epidemiology of nonalcoholic fatty liver disease-Meta-analytic assessment of prevalence, incidence, and outcomes. Hepatology 2016;64:73–84

8. Schmitz J, Evers N, Awazawa M, et al. Obesogenic memory can confer long-term increases in adipose tissue but not liver inflammation and insulin resistance after weight loss. Mol Metab 2016;5:328–339

9. Gavin JR, Alberti KGMM, Davidson MB, et al.; Expert Committee on the Diagnosis and Classification of Diabetes Mellitus. Report of the expert committee on the diagnosis and classification of diabetes mellitus. Diabetes Care 2000; 23(Suppl. 1):S4–S19

10. Brunt EM, Janney CG, Di Bisceglie AM, Neuschwander-Tetri BA, Bacon BR. Nonalcoholic steatohepatitis: a proposal for grading and staging the histological lesions. Am J Gastroenterol 1999;94:2467–2474

11. Brunt EM, Kleiner DE, Wilson LA, et al.; NASH Clinical Research NetworkA list of members of the Nonalcoholic Steatohepatitis Clinical Research Network can be found in the Appendix. Portal chronic inflammation in nonalcoholic fatty liver disease (NAFLD): a histologic marker of advanced NAFLD-Clinicopathologic correlations from the nonalcoholic steatohepatitis clinical research network. Hepatology 2009;49:809–820

12. Isakson P, Hammarstedt A, Gustafson B, Smith U. Impaired preadipocyte differentiation in human abdominal obesity: role of Wnt, tumor necrosis factor-alpha, and inflammation. Diabetes 2009;58:1550–1557

13. Al-Khalili L, Krämer D, Wretenberg P, Krook A. Human skeletal muscle cell differentiation is associated with changes in myogenic markers and enhanced insulin-mediated MAPK and PKB phosphorylation. Acta Physiol Scand 2004;180: 395–403

14. Hammarstedt A, Hedjazifar S, Jenndahl L, et al. WISP2 regulates preadipocyte commitment and PPARγ activation by BMP4. Proc Natl Acad Sci U S A 2013;110: 2563–2568

15. Johnson TO, Ermolieff J, Jirousek MR. Protein tyrosine phosphatase 1B inhibitors for diabetes. Nat Rev Drug Discov 2002;1:696–709

16. Verma M, Gupta SJ, Chaudhary A, Garg VK. Protein tyrosine phosphatase 1B inhibitors as antidiabetic agents - a brief review. Bioorg Chem 2017;70:267–283

17. Kleiner DE, Brunt EM, Van Natta M, et al.; Nonalcoholic Steatohepatitis Clinical Research Network. Design and validation of a histological scoring system for nonalcoholic fatty liver disease. Hepatology 2005;41:1313–1321

18. Arner P, Arner E, Hammarstedt A, Smith U. Genetic predisposition for Type 2 diabetes, but not for overweight/obesity, is associated with a restricted adipogenesis. PLoS One 2011;6:e18284

19. Smith U, Kahn BB. Adipose tissue regulates insulin sensitivity: role of adipogenesis, de novo lipogenesis and novel lipids. J Intern Med 2016;280:465–475

20. Lotta LA, Gulati P, Day FR, et al.; EPIC-InterAct Consortium; Cambridge FPLD1 Consortium. Integrative genomic analysis implicates limited peripheral adipose storage capacity in the pathogenesis of human insulin resistance. Nat Genet 2017; 49:17–26

21. Hocking S, Samocha-Bonet D, Milner K-L, Greenfield JR, Chisholm DJ. Adiposity and insulin resistance in humans: the role of the different tissue and cellular lipid depots. Endocr Rev 2013;34:463–500

22. Tchernof A, Després J-P. Pathophysiology of human visceral obesity: an update. Physiol Rev 2013;93:359–404
23. Goldstein BJ. Protein-tyrosine phosphatases: emerging targets for therapeutic intervention in type 2 diabetes and related states of insulin resistance. J Clin Endocrinol Metab 2002;87:2474–2480
24. Zabolotny JM, Kim Y-B, Welsh LA, Kershaw EE, Neel BG, Kahn BB. Protein-tyrosine phosphatase 1B expression is induced by inflammation in vivo. J Biol Chem 2008;283:14230–14241
25. Zinker BA, Rondinone CM, Trevillyan JM, et al. PTP1B antisense oligonucleotide lowers PTP1B protein, normalizes blood glucose, and improves insulin sensitivity in diabetic mice. Proc Natl Acad Sci U S A 2002;99:11357–11362
26. Brazil DP, Church RH, Surae S, Godson C, Martin F. BMP signalling: agony and antagony in the family. Trends Cell Biol 2015;25:249–264
27. Dutton LR, O'Neill CL, Medina RJ, Brazil DP. No evidence of Gremlin1-mediated activation of VEGFR2 signaling in endothelial cells. J Biol Chem 2019;294:18041–18045
28. Hoffmann JM, Grunberg JR, Hammarstedt A, et al. BMP4 gene therapy enhances insulin sensitivity but not adipose tissue browning in obese mice. Mol Metab 2020;32:15–26